

Supplementary Figures

Figure Legends

Supplementary Figure S1. Left panel shows western blots performed on HeLa cells 48 h after transient expression of PNKP-mGFP/mRFP (top), XRCC1-mGFP/mRFP (middle), and EGFP-FL LIG3/EGFP- Δ ZnF LIG3 (bottom). Right panel shows a schematic outline for all fluorescent proteins used in this study

Supplementary Figure S2. Cells co-expressing mGFP L360D (see Figure 2C) and WT XRCC1 mRFP were tested in different laser micro-irradiation systems (405-nm laser diode and multi-photon 750-nm). WT XRCC1 mRFP shows robust recruitment in response to both systems.

Supplementary Figure S3. Western blot showing PARP1 levels in PARP1 WT (F20) and null (A1) MEFs, where A549 lysate was used as a positive control.

Supplementary Figure S4. (A) Immunofluorescence staining, showing reduced formation of PAR following laser micro-irradiation in cells pretreated with AG14361. γ H2AX was used as a marker for DNA damage at laser tracks. (B) To ensure that the γ H2AX seen in the laser micro-irradiated tracks did not arise from stalled replication (i.e. conversion of SSB into DSB), non-synchronized HeLa cells transiently expressing mRFP-PCNA (marker for S-phase) were subjected to multi-photon 750-nm laser micro-irradiation as described in Materials and Methods (approximately 40 cells were analyzed). Subsequently (5-10 minutes post laser micro-irradiation) cells were fixed and stained for γ H2AX. A robust signal for γ H2AX was observed in all cells analyzed. A higher magnification of individual cells reveals PCNA distribution in S-phase (upper panel showing punctate PCNA distribution) and in non S-phase cells (lower panel showing a more homogeneous distribution of PCNA outside of the nucleoli). γ H2AX is detected in laser micro-IR tracks in S-phase and non S-phase cells. (C) Confirmation of the PARP inhibition results shown in Figure 5, using different PARP inhibitor, PJ-34. For recruitment curve, error bars represent S.E.M; $n=24$.

Supplementary Figure S5. Western blot showing the knock down of LIG3 by the Hush plasmid at different time points post transfection. Actin levels represent loading controls.

Supplementary Figure S6. Endogenous LIG3 shows robust accumulation at sites of DNA damage created by either (A) laser micro-irradiation or (B) by 10 mM H₂O₂ even upon pre-treatment of cells with 1 and 2 μ M AG14361. (C and D) LIG3 did not co-localize with γ H2AX (universal DSB marker) or 53BP1 (NHEJ DSB marker). For AG14361 treatments, cells were incubated with either 1 or 2 μ M drug at 37°C for 1-2 hours, then cells were either subjected to laser micro-irradiation (see Materials and Methods), or treated with 10 mM H₂O₂ for 10 minutes, then fixed and stained for immunofluorescence. We need to say something about the zoomed images in B and C

Supplementary Figure S7. FRAP analysis showing differences in binding kinetics in response to H₂O₂ damage between FL-LIG3 and Δ ZnF-LIG3. Error bars represent S.E.M; $n=24$.

Supplementary Figure S8. FRAP analysis showing the differences in binding kinetics of PARP1 in the presence and absence of DNA damage introduced by H₂O₂. Error bars represent S.E.M; $n=24$.

Figure S1

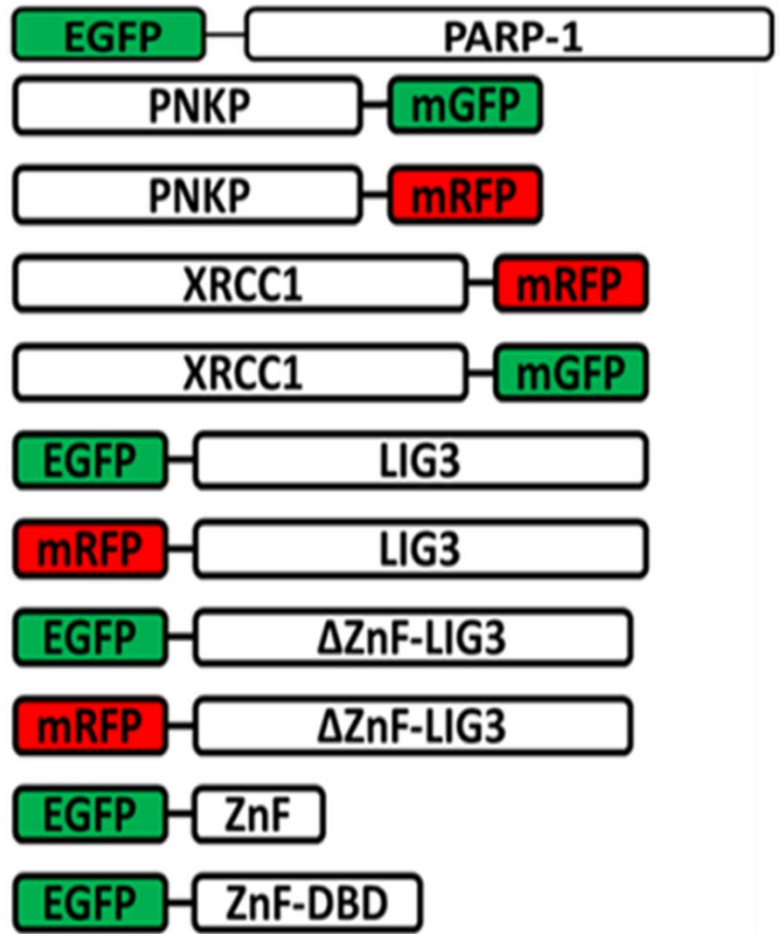
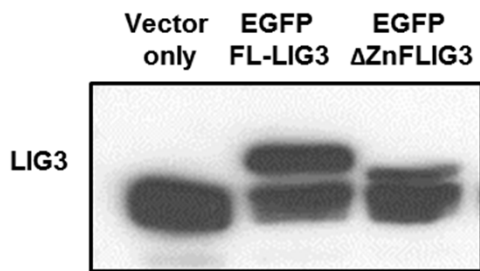
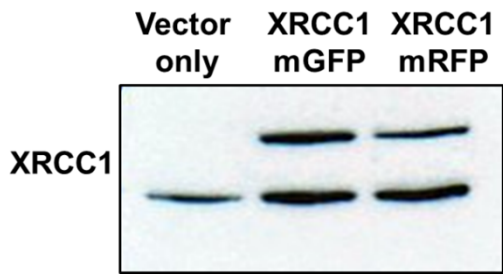
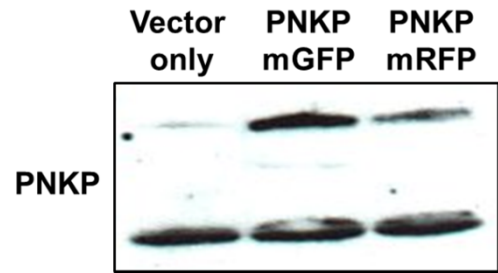


Figure S2

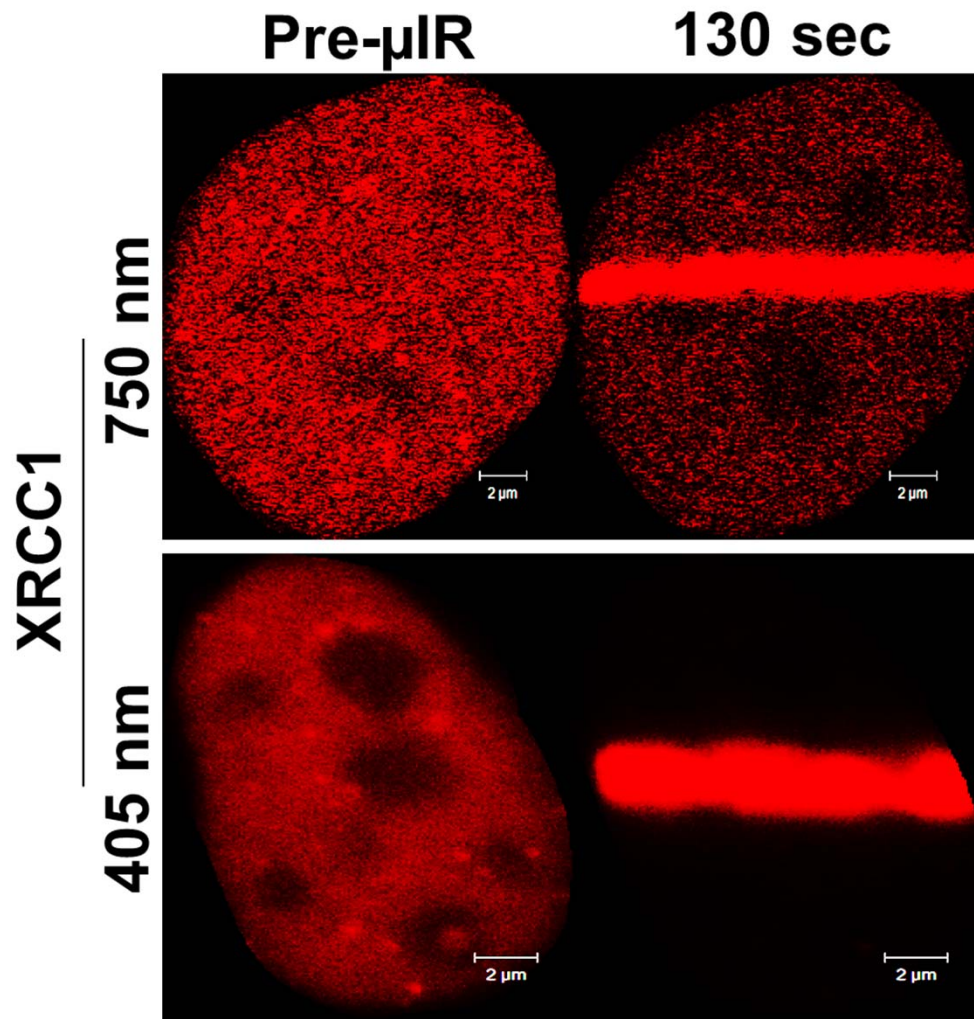


Figure S3

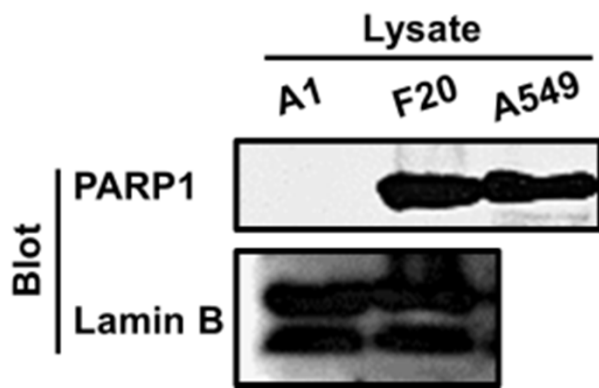
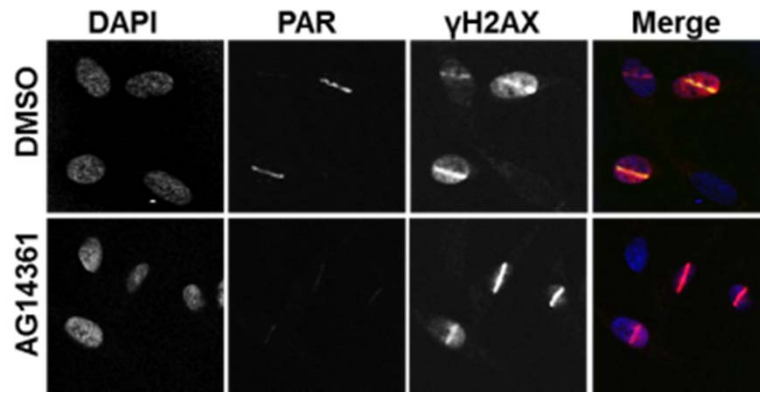
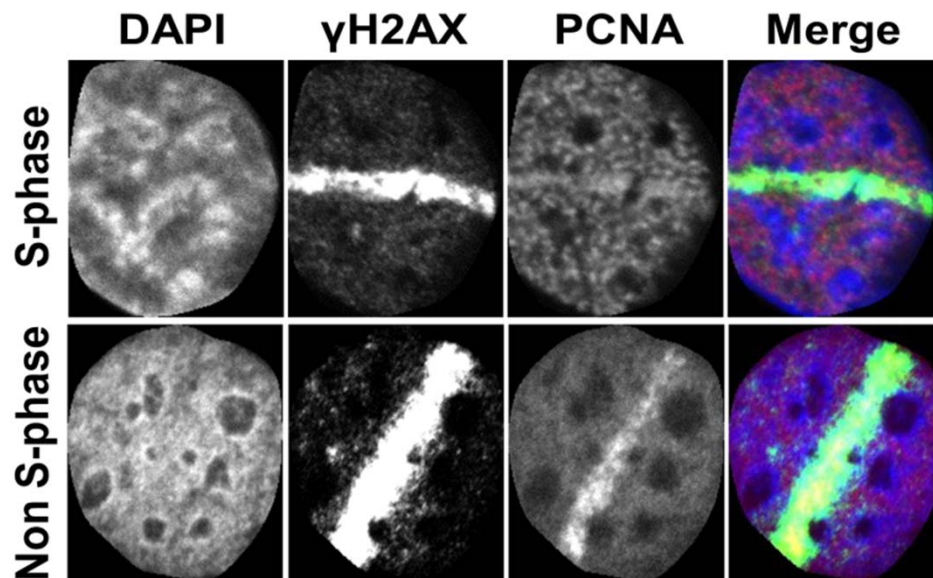
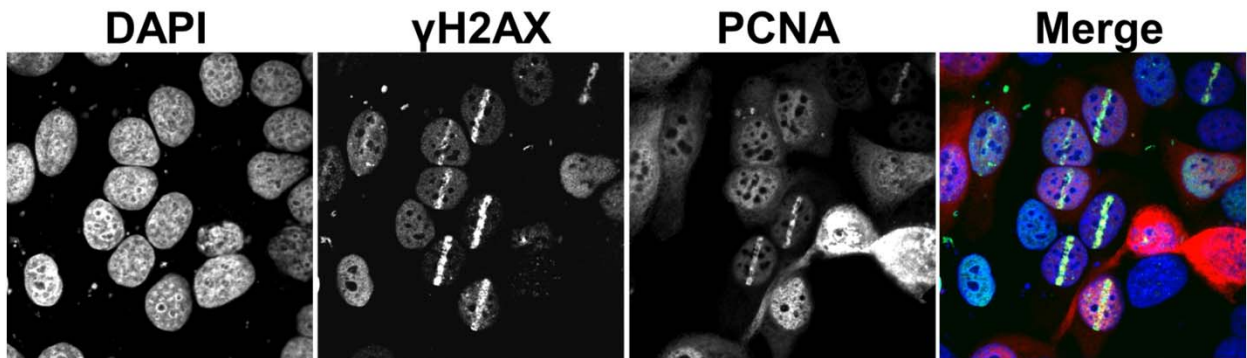


Figure S4

A)



B)



C)

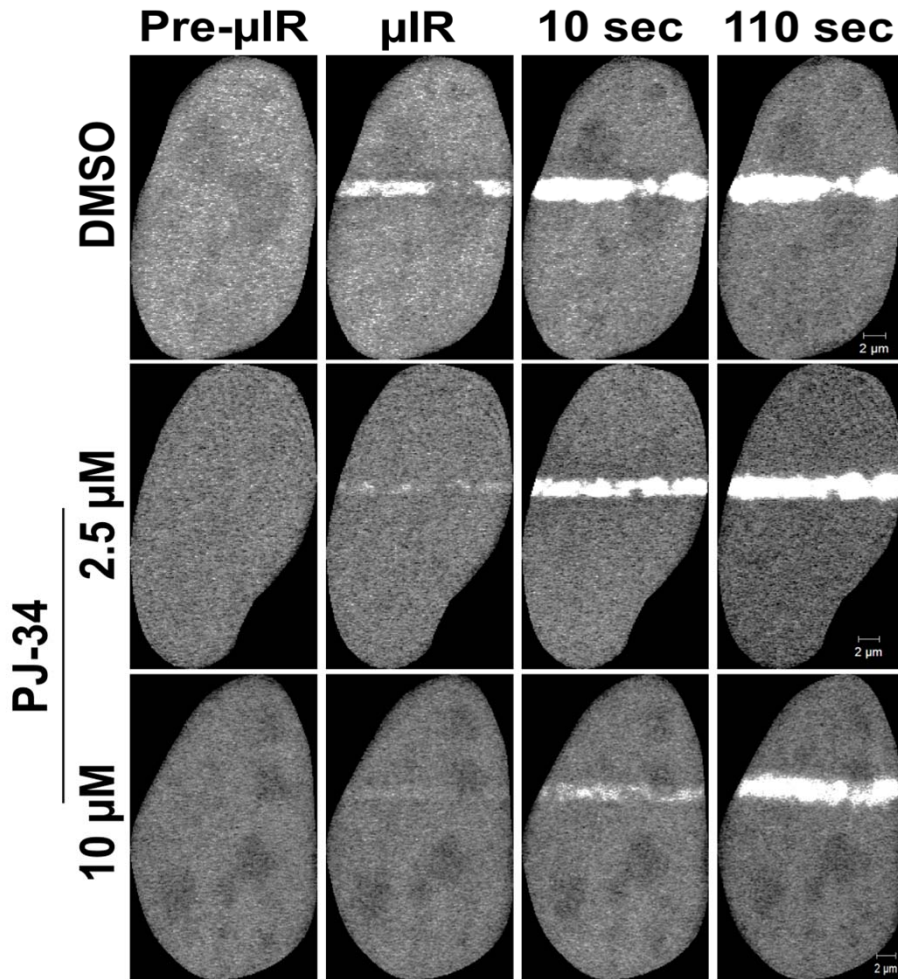
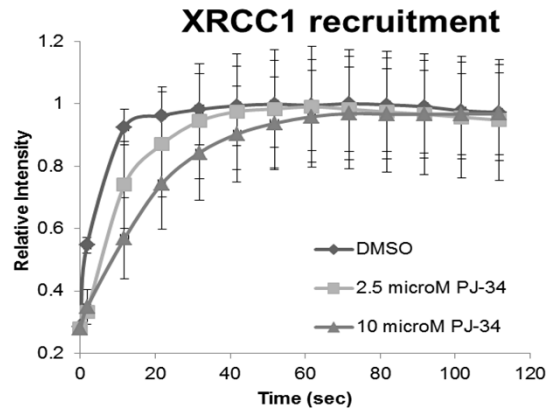


Figure S5

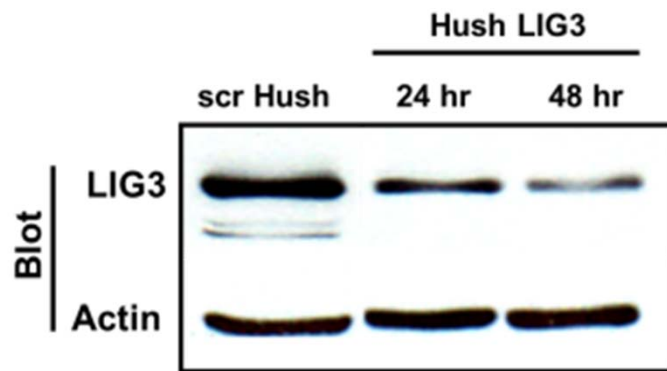
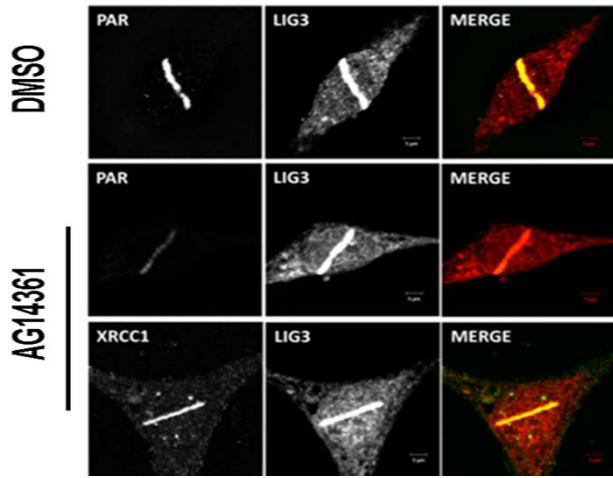
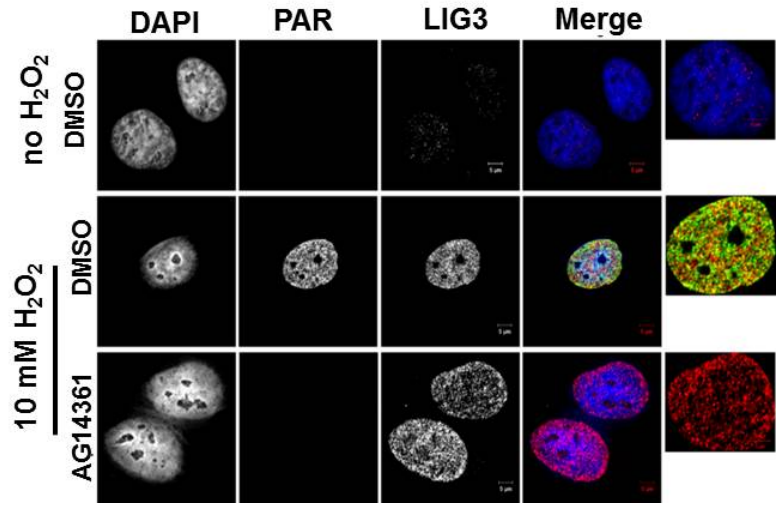


Figure S6

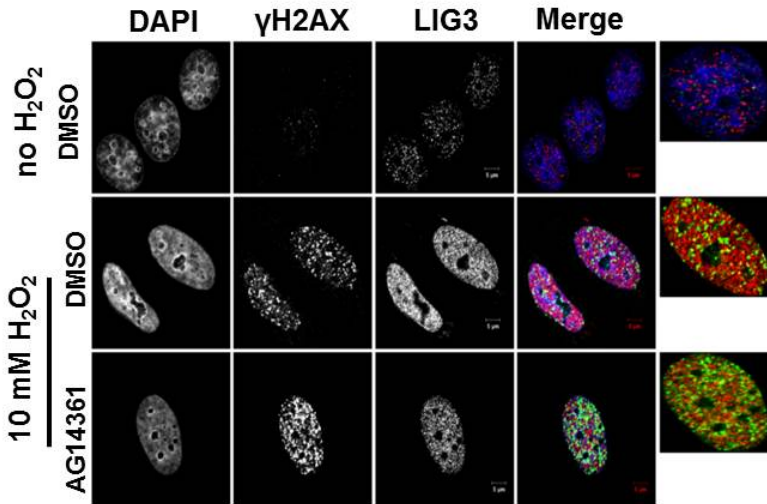
A)



B)



C)



D)

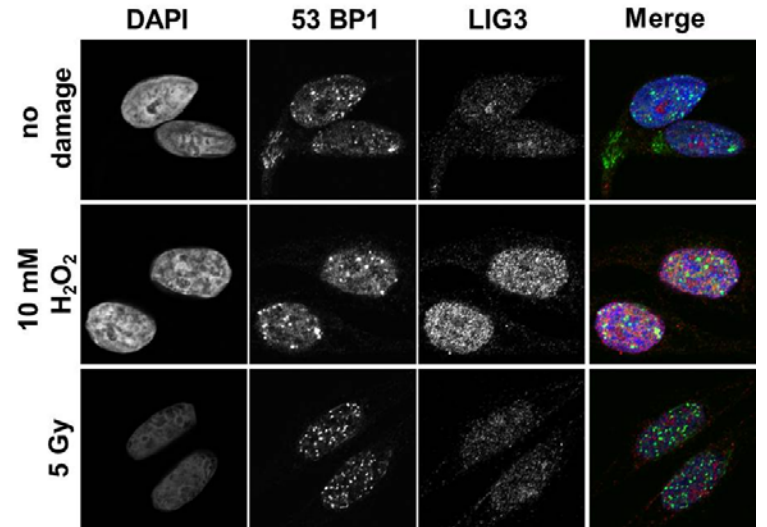


Figure S7

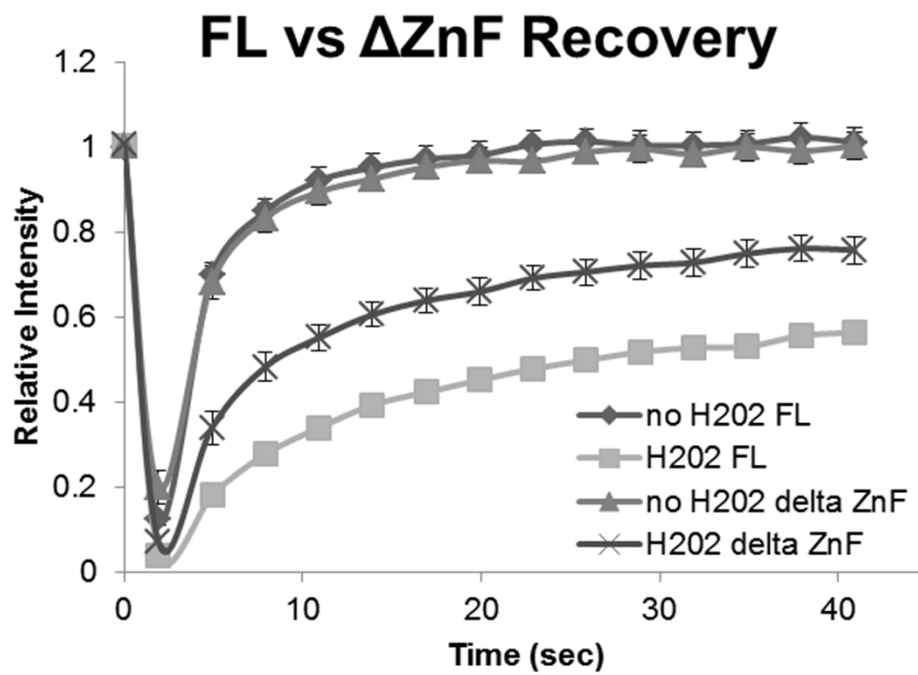


Figure S8

